Anti-Hepatic Fibrosis Mechanism of Lavandulyl Flavonoid KA from *Sophora flavescens* via TGF/Smad Signaling Pathway

Huang YANG, Xingjun CHEN, Yan LIN*

State Key Laboratory of Discovery and Utilization of Functional Components in Traditional Chinese Medicine, Guizhou Medical University, Guiyang 550025, China; Engineering Research Center of Authentic Medicinal Materials for Chronic Disease Prevention and Treatment under Guizhou Provincial Department of Education, Guiyang 550025, China

Abstract [**Objectives**] To investigate the anti-hepatic fibrosis mechanism of lavandulyl flavonoid Kurarinol A (KA) from *Sophora flavescens* through the TGF/Smad signaling pathway. [**Methods**] A hepatic fibrosis model was established by TGF-β1-induced activation of human hepatic stellate cells LX-2. Western blot and RT-qPCR techniques were employed to study the anti-fibrotic mechanism of KA through the TGF/Smad signaling pathway. [**Results**] KA exerted anti-hepatic fibrosis effects by significantly reducing the gene expression levels of TGF-β1, Smad2, Smad3, and Smad4, as well as markedly decreasing the protein expression levels of TGF-β1, p-Smad2/3/Smad2/3, and Smad4. [**Conclusions**] KA demonstrates significant anti-hepatic fibrosis activity and alleviates liver fibrosis through the TGF/Smad signaling pathway.

Key words *Sophora flavescens*, Kurarinol A (KA), TGF/Smad signaling pathway, Anti-hepatic fibrosis

1 Introduction

Sophora flavescens is a medicinal plant in the Leguminosae family[1]. In traditional Chinese medicine, *Sophora flavescens* has been widely used in combination with other medicinal plants to treat fever, dysentery, hematochezia, jaundice, oliguria, eczema, inflammatory diseases, and conditions related to skin burns[2]. It enhances liver function, reduces hepatotoxicity, exhibits antitumor effects, and protects the liver from hepatitis B infection and hepatic fibrosis. Alkaloids and flavonoids are the characteristic components found in *Sophora flavescens*[3]. Among these components, lavandulyl flavonoids have demonstrated promising antioxidant and anti-proliferative activity[4]. Moreover, our research group previously discovered the significant anti-inflammatory activity of lavandulyl flavonoids[5].

Hepatic fibrosis (HF) is a critical pathological condition occurring in many chronic liver diseases, caused by persistent liver injury and fibrotic scar formation. HF is characterized by excessive deposition of extracellular matrix (ECM) composed of cross-linked collagens (types I and III), fibronectin, elastin fibers, glycoproteins, and mucopolysaccharides, which disrupts liver structure and function[6]. Without intervention, hepatic fibrosis can progress to cirrhosis, liver failure, or hepatocellular carcinoma, imposing a substantial global health burden. Therefore, effective therapies for hepatic fibrosis are urgently needed[7]. Current studies have confirmed that total flavonoids from *Sophora flavescens* can inhibit collagen deposition and hepatic fibrosis in rats through antioxidative stress mechanisms.

Hepatic stellate cells (HSCs) are the primary cellular source of extracellular matrix production during liver injury. The activation and transformation of HSCs into myofibroblast-like cells constitute a central process in the initiation and progression of hepatic fibrosis. Under normal circumstances, activated HSCs either undergo apoptosis or are inactivated through unknown regulatory mechanisms, thereby controlling fibrosis. When this balance is disrupted, persistently activated HSCs drive uncontrolled fibrogenesis, leading to progressive fibrosis, structural and functional alterations, and ultimately cirrhosis and liver cancer[8].

Multiple signaling pathways are involved in the development of hepatic fibrosis, primarily including TGF-β/Smad, TLRs/NF-κB, PI3K/Akt, glycolysis, and lipid metabolism pathways[9-12]. The Toll-like receptor signaling pathway is most closely associated with inflammation[10]. The Toll-like receptors (TLRs), as key components of the innate immune system, serve as primary regulators of hepatic inflammatory responses and play crucial roles in the pathogenesis and progression of liver fibrosis. The TLR family contains multiple subtypes (TLR2-TLR9), with several TLRs participating in the formation and progression of hepatic fibrosis. TLR4, as a major TLR-related protein, activates hepatic inflammatory responses upon stimulation, particularly by inducing nuclear factor-κB (NF-κB) in the pathway to amplify liver inflammation, regulate HSC proliferation, and promote excessive ECM secretion, ultimately leading to hepatic fibrosis. Studies have shown that individual knockout of TLR2, TLR4, TLR5, or TLR9 genes cannot completely suppress carbon tetrachloride-induced hepatic fibrosis in mice[13-16]. This suggests that TLR2, TLR4, TLR5, and TLR9 in the TLRs/NF-κB inflammatory signaling pathway

Received: February 13, 2025 Accepted: May 26, 2025
Supported by Guizhou Provincial Science and Technology Project (2024-023; ZK2024-047, 2024-015); the Innovation and Entrepreneurship Training Program for Undergraduates from China (202310660082, S2024106601432X); University Engineering Research Center for the Prevention and Treatment of Chronic Diseases by Authentic Medicinal Materials in Guizhou Province (2023-035); Administration of Traditional Chinese Medicine of Guizhou Province (QZYY-2024-134); Science Foundation of the Health Commission of Guizhou Province (gzwkj2025-538).

* Corresponding author. Yan LIN, associate professor.

may not be direct therapeutic targets for anti-fibrotic interventions.

Therefore, this study employed transforming growth factor-β1 (TGF-β1)-induced human hepatic stellate cells LX-2 to establish an *in vitro* hepatic fibrosis model. RT-qPCR and Western blot techniques were utilized to investigate the effects of Kurarinol A (KA), a lavandulyl flavonoid isolated from the ethyl acetate inhibitory fraction of *Sophora flavescens*, on the expression of TGF/Smad signaling pathway-related molecules in activated LX-2 cells.

2 Materials and methods

2.1 Instruments Ultrahigh-speed refrigerated centrifuge (Optima XPN-100, Beckman Coulter, USA); Nucleic acid/protein analyzer (NanoDrop 2000, Thermo Fisher, USA); Real-time PCR system (CFX96 Touch, Bio-Rad, USA); Electrophoresis apparatus (PowerPac Basic, Bio-Rad, USA); Chemiluminescence imaging system (Azure c600, Azure Biosystems, USA); Cell incubator (Forma Steri-Cycle, Thermo Fisher, USA).

2.2 Reagents and materials

2.2.1 Reagents. TRIzol reagent (Invitrogen, Thermo Fisher, USA); Reverse transcription kit (Promega, USA); SYBR Green PCR Master Mix (Applied Biosystems, Thermo Fisher, USA); Rabbit anti-human TGF-β1 monoclonal antibody, rabbit anti-human Smad2/3 monoclonal antibody, rabbit anti-human Smad4 monoclonal antibody (Wuhan SanYing Biotechnology, China); Mouse anti-human GAPDH monoclonal antibody, mouse anti-human β-actin monoclonal antibody, DMSO, lipopolysaccharide (LPS) (Sigma-Aldrich, USA); HRP-conjugated goat anti-rabbit IgG antibody, HRP-conjugated goat anti-mouse IgG antibody (Jackson ImmunoResearch, USA); Cell culture medium, fetal bovine serum, penicillin-streptomycin solution (Gibco, Thermo Fisher, USA).

2.2.2 Experimental cells. Human hepatic stellate cells LX-2 were purchased from Procell Life Science & Technology Co., Ltd, and cultured in DMEM medium containing 10% fetal bovine serum and 1% penicillin-streptomycin solution, maintained at 37 ℃ in a 5% CO_2 incubator.

2.3 Preparation of drugs and reagents

2.3.1 Preparation of experimental drug. An appropriate amount of Kurarinol A (KA) was dissolved in DMSO to prepare a 10 mM stock solution stored at −20 ℃. The stock solution was diluted with serum-free medium to desired concentrations before use.

2.3.2 Preparation of 1 × PBS buffer. 8 g of NaCl, 0.2 g of KCl, 1.44 g of Na_2HPO_4 and 0.24 g of KH_2PO_4 were dissolved in 800 mL of distilled water. The pH was adjusted to 7.4 using HCl, followed by dilution to 1 L with distilled water. The solution was autoclaved and stored at 4 ℃.

2.4 Cell culture LX-2 cells were thawed and seeded in culture flasks. When reaching 80% −90% confluence, cells were digested with 0.25% trypsin for subculture. Experimental groups included: normal control group, model group (TGF-β1-induced activation), positive drug group (silibinin, 60 μM), and KA treatment group (2.5, 5, 10 μM).

2.5 Total RNA extraction from LX-2 cells LX-2 cells in logarithmic growth phase were collected and gently washed twice with pre-cooled PBS. 1 mL of TRIzol reagent was added to each well to ensure complete cell lysis, followed by 5-min incubation at room temperature. After adding 0.2 mL of chloroform, the mixture was vigorously shaken for 15 s and allowed to stand for 2 −3 min. The mixture was centrifuged at 12 000 rpm for 15 min at 4 ℃. The upper aqueous phase was carefully transferred to a new tube. 0.5 mL of isopropyl alcohol was added, mixed gently, and incubated for 10 min at room temperature. After centrifugation at 12 000 rpm for 10 min at 4 ℃, the supernatant was discarded. RNA pellets were washed twice with 75% ethanol. Air-dried RNA pellets were dissolved in DEPC-treated water, and RNA concentration/purity was determined using NanoDrop 2000.

2.6 RT-qPCR 1 μg of total RNA was reverse-transcribed into cDNA using the reverse transcription kit according to manufacturer's instructions. Real-time PCR amplification was performed using SYBR Green PCR Master Mix with cDNA as template. Primer sequences were as Table 1.

Table 1 Primer sequences for RT-qPCR analysis

Gene	Forward	Reverse
GAPDH	GGAGTCCACTGGCGTCTTCAC	GCTGATGATCTTGAGGCTGTTGTC
TGF-β1	AGCAACAATTCCTGGCGATACCTC	TCAACCACTGCCGCACAACTC
Smad2	CCTGCTCCTGACCACAACTCTG	TCATCCCTTCCCACCCACTCC
Smad3	AGGCTGCTTGTAGGACTGTTCAC	CGCTGTGTTGAGGTTTGGTTCTG
Smad4	AGGATCAGTAGGTGGAATAG	TCTAAAGGTTGTGGGTCTGC
TLR4	GCTCTTGGTGGAAGTTGAACGAATG	CAAGCACACTGAGGACCGACAC
MyD88	GCCGCCTGTCTCTGTTCTTG	GTCCGCTTGTGTCTCCAGTTG
TRAF6	TGTGCCTCTGCTCTTACTGTCTG	GAACTATGGTCACTGCTGCTTGG
TIRAP	GGCAAGATGGCTGACTGGTTC	GGTAGTGGGCTGTCCTGTGAG
TAK1	AGACAATGGAATTAGGGCAGGTTTG	GACGGAAGGCAGGCAACAATC
NF-κB	ATGGTGGTCGGCTTCGCAAAC	CGCCTCTGTCATTCGTGCTTCC
TNF-α	AAGGACACCATGAGCACTGAAAGC	AGGAAGGAGAAGAGGCTGAGGAAC
IL-1β	GGACAGGATATGGAGCAACAAGTGG	CAACACGCAGGACAGGTACAGATTC

Reaction conditions: 95 ℃ pre-denaturation for 3 min; 40 cycles of 95 ℃ denaturation for 15 s, 60 ℃ annealing for 30 s, and 72 ℃ extension for 30 s. GAPDH was used as internal reference, and relative gene expression was calculated using the $2^{-\Delta\Delta Ct}$ method.

2.7 Western blot Cells were collected and washed twice with pre-cooled PBS. Appropriate amount of protein lysis buffer was added, and cells were lysed on ice for 30 min. After centrifugation at 12 000 rpm for 15 min at 4 ℃, supernatants were collected. Protein concentration was determined using BCA method. Equal amounts of protein samples were mixed with 5 × SDS loading buffer and denatured by boiling for 5 min.

After denaturation, SDS-PAGE electrophoresis was performed. Proteins were transferred to PVDF membranes, which were blocked with 5% skim milk for 2 h. Membranes were incubated overnight at 4 ℃ with rabbit anti-human TGF-β1 monoclonal antibody (1 ∶ 1 000), rabbit anti-human Smad2/3 monoclonal antibody (1 ∶ 1 000), rabbit anti-human Smad4 monoclonal antibody (1 ∶ 1 000), and mouse anti-human GAPDH monoclonal antibody (1 ∶ 5 000).

The next day, membranes were washed three times with TBST (10 min each). HRP-conjugated goat anti-rabbit IgG antibody (1 ∶ 5 000) and HRP-conjugated goat anti-mouse IgG antibody (1 ∶ 5 000) were added for 1-hour incubation at room temperature. After three additional TBST washes, bands were visualized using chemiluminescence imaging system. Band intensities were analyzed using ImageJ software, with β-actin as internal reference for calculating relative protein expression.

2.8 Statistical analysis Statistical analysis was performed using GraphPad Prism 8 software. Measurement data were expressed as mean ± standard deviation. One-way analysis of variance (ANOVA) was used for multi-group comparisons, followed by Tukey's test for pairwise comparisons. A P-value < 0.05 was considered statistically significant.

3 Results and analysis

3.1 RT-qPCR analysis of mRNA expression levels of TGF-β1, Smad2, Smad3, and Smad4 As shown in Fig. 1, RT-qPCR results indicated that mRNA expression levels of TGF-β1, Smad2, Smad3, and Smad4 were significantly elevated in the model group compared to the normal group, confirming successful establishment of the hepatic fibrosis model. Compared to the model group, KA treatment group (2.5, 5, 10 μM) exhibited significant reductions in mRNA expression levels of TGF-β1, Smad2, Smad3, and Smad4 (P < 0.05), with a clear dose-dependent trend. These findings preliminarily demonstrate that KA exerts anti-fibrotic effects at the genetic level by downregulating mRNA expression of TGF-β1, Smad2, Smad3, and Smad4 via the TGF/Smad signaling pathway.

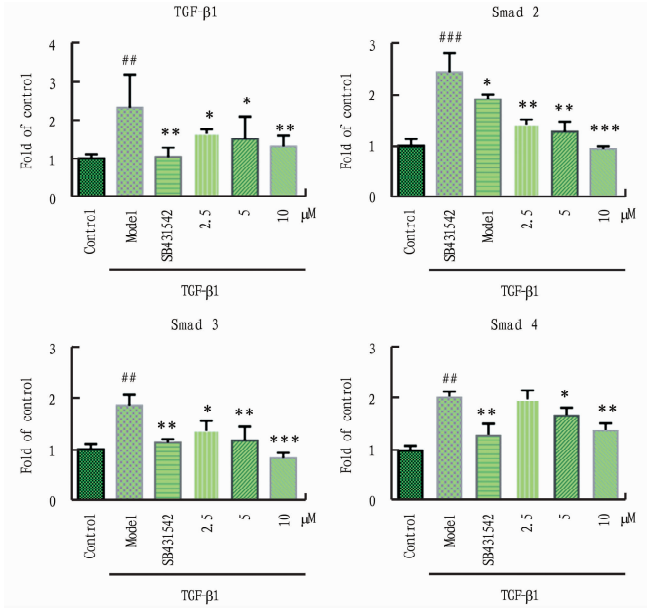

Fig. 1 mRNA expression levels of TGF-β1, Smad2, Smad3, and Smad4 detected by RT-qPCR

3.2 Western blot analysis of protein expression levels of TGF-β1, Smad2, Smad3, and Smad4 Western blot results (Fig. 2) revealed significantly increased protein expression levels of TGF-β1, p-Smad2/3/Smad2/3, and Smad4 in the model group compared to the normal group, further validating the successful induction of hepatic fibrosis. Compared to the model group, KA treatment group (2.5, 5, 10 μM) showed marked reductions in protein expression of TGF-β1, p-Smad2/3/Smad2/3, and Smad4 (P < 0.05) in a dose-dependent manner. These results further indicate that KA attenuates hepatic fibrosis at the protein level by suppressing TGF-β1, p-Smad2/3/Smad2/3, and Smad4 expression via the TGF/Smad signaling pathway.

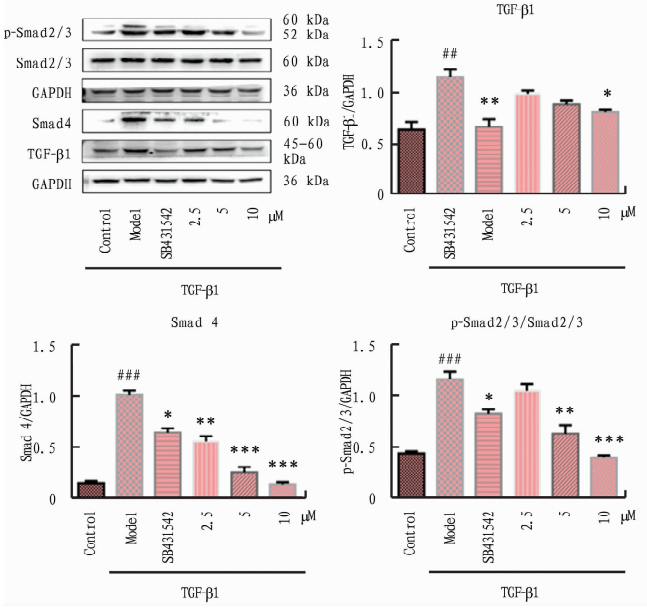

Fig. 2 Protein expression levels of TGF-β1, p-Smad2/3/Smad2/3, and Smad4 detected by Western blot

4 Conclusion

This study employed a TGF-β1-induced LX-2 cell activation model to investigate the anti-fibrotic mechanism of KA via the TGF/Smad signaling pathway using RT-qPCR and Western blot. The results demonstrate that KA alleviates hepatic fibrosis by significantly suppressing both gene expression levels (TGF-β1, Smad2, Smad3, Smad4) and protein expression levels (TGF-β1, p-Smad2/3/Smad2/3, Smad4), highlighting its therapeutic potential through modulation of the TGF/Smad pathway.

References

[1] WU X, LI L, JINHABURE, *et al.* Radix Sophorae Flavescentis of *Sophora flavescens* Aiton inhibits LPS-induced macrophage pro-inflammatory response via regulating CFHR2 expression[J]. Journal of Ethnopharmacology, 2024, 331: 118210.

[2] HE X, FANG J, HUANG L, *et al.* *Sophora flavescens* Ait.: Traditional usage, phytochemistry and pharmacology of an important traditional Chinese medicine[J]. Journal of Ethnopharmacology, 2015, 172: 10 – 29.

[3] YANG H, ZHOU Z, HE L, *et al.* Hepatoprotective and inhibiting HBV effects of polysaccharides from roots of *Sophora flavescens*[J]. International Journal of Biological Macromolecules, 2018, 108: 744 – 752.

[4] ABOALHAIJA NH, SYAJ H, AFIFI F, *et al.* Chemical evaluation, *in vitro* and *in vivo* anticancer activity of *Lavandula angustifolia* grown in Jordan[J]. Molecules, 2022, 27(18): 5910.

[5] LI JJ, ZHANG X, SHEN XC, *et al.* Phytochemistry and biological properties of isoprenoid flavonoids from *Sophora flavescens* Ait.[J]. Fitoterapia, 2020, 143: 104556.

[6] HU Y, ZHANG Z, ADIHAM A, *et al.* *In vivo* and *in vitro* models of hepatic fibrosis for pharmacodynamic evaluation and pathology exploration [J]. International Journal of Molecular Sciences, 2025, 26(2): 696.

[7] XIONG Z, CHEN P, WANG Z, *et al.* Human umbilical cord-derived mesenchymal stem cells attenuate liver fibrosis by inhibiting hepatocyte ferroptosis through mitochondrial transfer[J]. Free Radical Biology and Medicine, 2025, 231: 163 – 177.

[8] BANERJEE A, FARCI P. Fibrosis and hepatocarcinogenesis: Role of gene-environment interactions in liver disease progression[J]. International Journal of Molecular Sciences, 2024, 25(16): 8641.

[9] ZHANG TZ, HE XL, CALDWELL L, *et al.* NUAK1 promotes organ fibrosis via YAP and TGF-β/Smad signaling[J]. Science Translational Medicine, 2022, 14(637): eaaz4028.

[10] HAMMERICH L, TACKE F. Hepatic inflammatory responses in liver fibrosis[J]. Nature Reviews Gastroenterology & Hepatology, 2023, 20: 633 – 646.

[11] YANG X, LI Q, LIU WT, *et al.* Mesenchymal stromal cells in hepatic fibrosis/cirrhosis: From pathogenesis to treatment[J]. Cellular & Molecular Immunology, 2023, 20(6): 583 – 599.

[12] KIM DH, PARK JS, CHOI HI, *et al.* The role of the farnesoid X receptor in kidney health and disease: A potential therapeutic target in kidney diseases[J]. Experimental & Molecular Medicine, 2023, 55: 304 – 312.

[13] WANG Z, CHENG ZX, ABRAMS ST, *et al.* Extracellular histones stimulate collagen expression *in vitro* and promote liver fibrogenesis in a mouse model via the TLR4-MyD88 signaling pathway[J]. World Journal of Gastroenterology, 2020, 26(47): 7513 – 7527.

[14] SOARES JB, PIMENTEL-NUNES P, AFONSO L, *et al.* Increased hepatic expression of TLR2 and TLR4 in the hepatic inflammation-fibrosis-carcinoma sequence[J]. Innate Immunity, 2012, 18(5): 700 – 708.

[15] WATANABE A, HASHMI A, GOMES D A, *et al.* Apoptotic hepatocyte DNA inhibits hepatic stellate cell chemotaxis via toll-like receptor 9[J]. Hepatology, 2007, 46(5): 1509 – 1518.

[16] GÄBELE E, MÜHLBAUER M, DORN C, *et al.* Role of TLR9 in hepatic stellate cells and experimental liver fibrosis[J]. Biochemical and Biophysical Research Communications, 2008, 376(2): 271 – 276.

(From page 25)

[3] XU JZ, WANG XQ, HUANG KX, *et al.* Studies on the chemical constituents of triterpenoid saponins in *Hemsleya chensnsis* Cogn[J]. Chinese Pharmaceutical Journal, 2022, 43(23): 1770 – 1773. (in Chinese).

[4] CHEN XY. Is traditional Chinese medicine toxic? It depends on how you use it[J]. World of Health, 2021 (8): 40 – 42. (in Chinese).

[5] HONG H, DU WF, ZHU WH, *et al.* Research progress on organ toxicity of traditional Chinese medicine[J]. China Journal of Traditional Chinese Medicine and Pharmacy, 2021, 36(2): 943 – 946. (in Chinese).

[6] PAN HL, PAN WJ, CHEN CY, *et al.* Research progress on the effects of active components of traditional Chinese medicine on liver toxicity[J]. Journal of Clinical Rational Drug Use, 2020, 13(27): 179 – 181. (in Chinese).

[7] LIU Y, CHEN S, ZHAO L. Study on drug-induced oxidative stress and hepatotoxicity in mice[J]. Chinese Journal of Modern Applied Pharmacy, 2022, 39(3): 261 – 267. (in Chinese)

[8] CEN LY, HUANG XQ, WANG YY, *et al.* Expression of PINK1/Parkin in peripheral blood of patients with SAP and its correlation with apoptosis factors[J]. Journal of Youjiang Medical University for Nationalities, 2023, 45(6): 842 – 847. (in Chinese).

[9] PENG ZX. Study on the dynamic changes of pulmonary surfactant in lung injury based on Wei-Qi-Ying-Xue syndrome differentiation[D]. Guangzhou: Guangzhou University of Chinese Medicine, 2012. (in Chinese).

[10] SU L, HUANG LZ, CAI Y. Preliminary study on the analgesic, anti-inflammatory and anti-acute liver injury effects of the water extract from Zhuang medicine *Munronia delavayi* Franch[J]. Journal of Youjiang Medical University for Nationalities, 2021, 43(6): 741 – 745. (in Chinese).

[11] DENG XH, LI YQ, ZHANG TT. Study on drug-induced inflammatory response and liver injury in mice[J]. Pharmacology and Clinics of Chinese Materia Medica, 2021, 37(6): 77 – 82. (in Chinese).

[12] WU Y, XU Y, WU L, *et al.* A review of adverse drug reactions and toxicity studies of Psoraleae Fructus[J]. Pharmacology and Clinics of Chinese Materia Medica, 2021, 37(6): 207 – 213. (in Chinese).